A Microstrip Three-Port and Four-Channel Multiplexer for WLAN and UWB Coexistence

Ming-Iu Lai, *Student Member, IEEE,* and Shyh-Kang Jeng, *Senior Member, IEEE*

***Abstract*—This paper proposes a microstrip three-port four-channel multiplexer for wireless systems where wireless local area network (WLAN) and ultra-wideband (UWB) coexist. The proposed multiplexer has two channels, from 2.15 to 2.89 GHz and from 5.13 to 5.84 GHz, for WLAN and two channels, from 3.22 to 4.83 GHz and from 6.07 to 8.22 GHz, for UWB. The measured scattering parameters agree well with the simulations. To determine a proper circuit topology and overcome the interference problems between ports, the genetic algorithm (GA) technique is exploited. The GA search takes approximately 3 min on a personal computer with a 2.4-GHz microprocessor. Additionally, the analysis of the circuit behaviors, the problem on the size of the multiplexer, and the isolation issues between WLAN and UWB ports are discussed.**

***Index Terms*—Genetic algorithm (GA), microstrip.**

I. Introduction

AFTER THE Federal Communications Commission (FCC) allocated the 3.1–10.6-GHz spectra for unlicensed use, the ultra-wideband (UWB) technology is emerging as a promising solution to a set of devices requiring data rates greater than 100 Mb/s for wireless personal-area network (WPAN) communications. In the near future, the notebooks, handheld, and consumer devices will be required to build the wireless local-area network (WLAN) and UWB radio transceivers in order to support various wireless functions. The spectra for these systems are plotted in Fig. 1. For the WLAN systems, it works on 2.4- and 5.0-GHz bands, which are commonly used all over the world. For WPAN communications, there are two candidates for the UWB systems, multiband orthogonal frequency division multiplexing (MB-OFDM) and direct-sequence spread-spectrum (DS-SS) [1]. The MB-OFDM UWB system divides the overall spectrum into 13 bands and four groups where Groups B and D are reserved for future use. The DS-SS UWB system based on impulse radio technology divides the spectrum into low-band and high-band. They keep away from WLAN signals on 5.0-GHz band as much as possible to avoid the undesired interferences between the two systems.

To setup a device consisting of both WLAN and UWB communication systems, a direct solution is based on a two-antenna configuration, as shown in Fig. 2. However, antennas may be too bulky, which is impractical for portable wireless facilities. Driven by the demand for the small-size and low-cost wireless facilities, a single-antenna configuration is a good choice for wireless systems where WLAN and UWB coexist, as shown in Fig. 3. The antennas are replaced by one UWB antenna covering both of the WLAN and UWB spectra and one three-port four-channel multiplexer with two channels for the WLAN and two channels for UWB. Numerous authors have reported various UWB antennas satisfying the desired bandwidth [3], [4] and, therefore, the three-port and four-channel multiplexer is a crucial key to the success of the single-antenna configuration.

The design of such a multiplexer presents many tough challenges. Almost all of the traditional methods used for duplexer or multiplexer design [5]–[11] focused on the narrow-band case and that one port is only with one channel. An intuitive design is to accomplish four single-band bandpass filters or two dual-band bandpass filters and then connect filters together [12], [13], as shown in Fig. 4(a) and (b). For such an architecture,

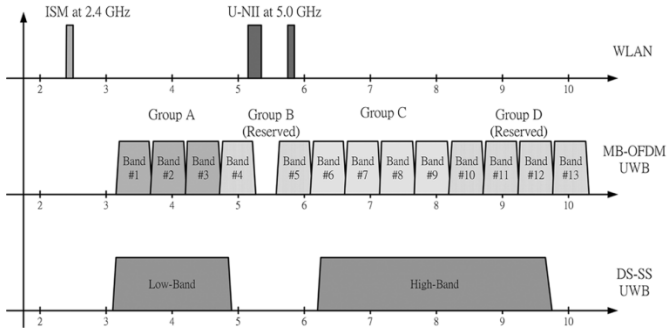

Fig. 1. Allocated spectra for WLAN and UWB.

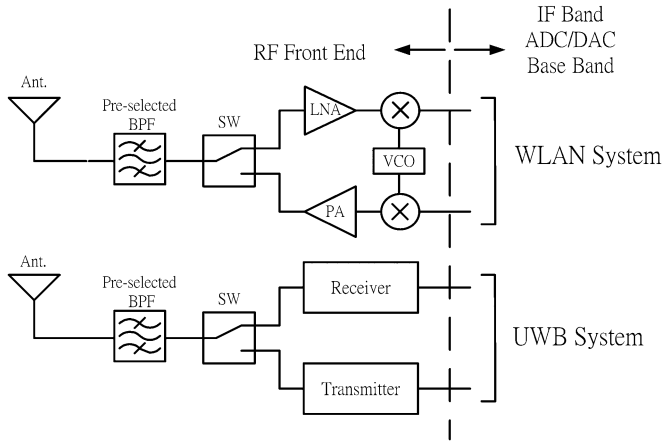

Fig. 2. Two-antenna configuration for WLAN and UWB coexistence.

Manuscript received April 7, 2005. This work was supported by the National Science Council, Taiwan, R.O.C., under Grant NSC 93-2213-E-002-091 and the Department of Industrial Technology, Ministry of Economic Affairs, R.O.C., under Technology Development Program of Academic 93-EC-17-A-05-S1-020.

The authors are with the Graduate Institute of Communication Engineering and Department of Electrical Engineering, National Taiwan University, Taipei, 10617 Taiwan, R.O.C. (e-mail: skjeng@ew.ee.ntu.edu.tw).

Digital Object Identifier 10.1109/TMTT.2005.855136

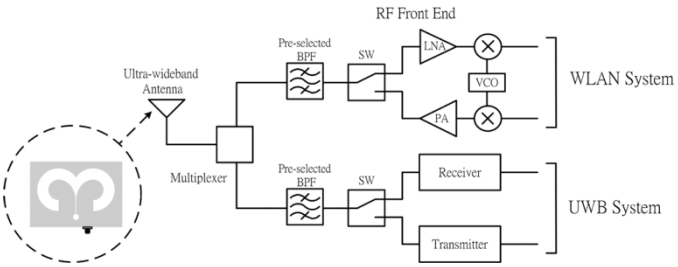

Fig. 3. Single-antenna configuration for WLAN and UWB coexistence.

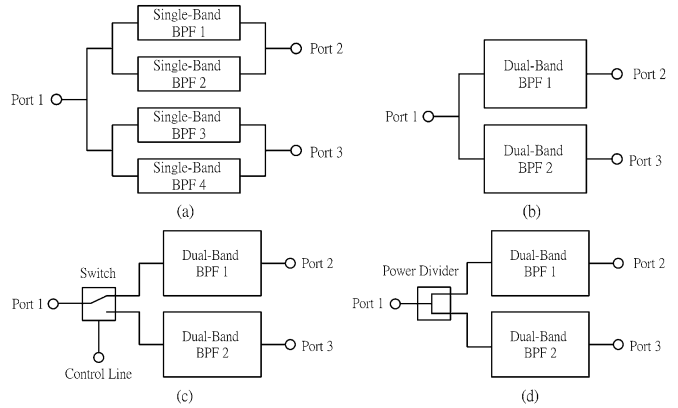

Fig. 4. Multiplexer architectures. (a) Using four single-band bandpass filters. (b) Using two dual-band bandpass filters. (c) Using a switch to connect two dual-band bandpass filter. (d) Using a power divider to connect two dual-band bandpass filter.

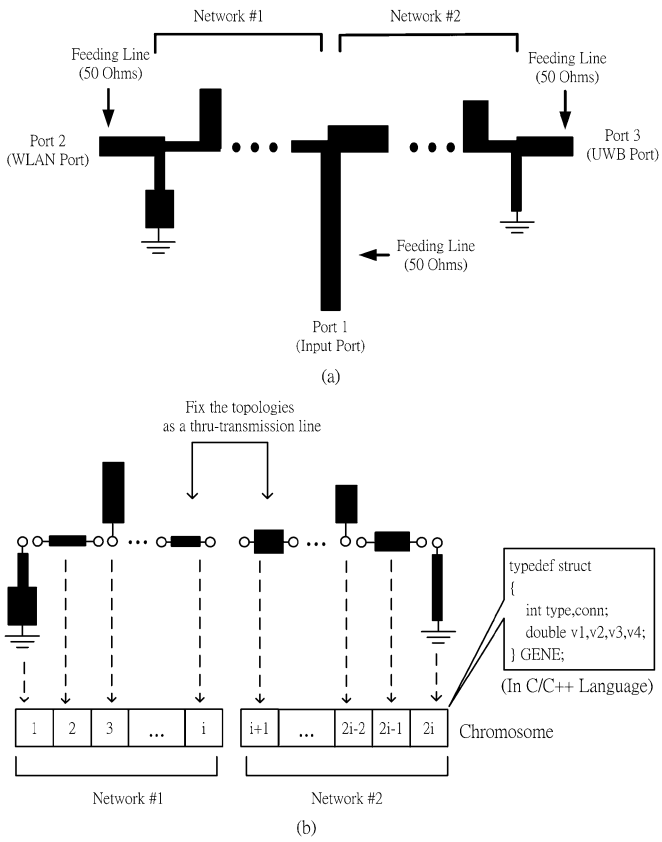

Fig. 5. Representation scheme in the proposed algorithm. (a) A typical passive microstrip circuit. (b) Decomposition of the circuit in (a) into basic circuit elements.

some unwanted interactions between the filters may cause serious degradation of passbands and stopbands. Another possible approach is to combine the filters using either a switch or power divider [14], as shown in Fig. 4(c) and (d). The solution with a switch is not cost effective because it requires an UWB switch and additional control circuitries. For the power-divider solution, each channel is subject to the additional 3-dB loss and the design of an UWB power divider presents other thorny problems.

In this paper, the Fig. 4(b) architecture is chosen to design the desired multiplexer. The topology of the dual-band bandpass filters is similar to that of dual-behavior resonator (DBR) filters [15]–[17], which are filters with dual-band characteristics by controlling the harmonic response. To determine a proper circuit topology and overcome the interference problems between ports, the genetic algorithm (GA) technique [18]–[21] is used. More details are presented in Section II. In Section III, we implement a three-port and four-channel multiplexer with a microstrip line and present the simulated and measured frequency responses. Section IV presents discussions including the analysis of circuit behaviors, the size problem, and the isolation issues of the multiplexer. Finally, brief conclusions are given in Section IV.

II. Design Methodology

To enable a GA algorithm to search for not only electrical parameters, but also the circuit topology, first of all, we have to propose a special representation scheme that is capable of describing all circuit information. As illustrated in Fig. 5, a multiplexer circuit consisting of many open- and short-circuited stubs can be decomposed into basic circuit elements. The data structure shown in Fig. 5(b) is then applied to describe a basic circuit element. It is composed of three parts. The first part is an integer representing the topology of a basic element. The second part is an integer representing the way of connection to the previous element. The third part is a set of real numbers describing the corresponding electrical parameters of the element. Table I lists the details of the basic circuit elements. A special gene called *Empty* is introduced, which enables the representation scheme to describe a circuit with an arbitrary number of basic circuit elements and circuit orders. In a chromosome with $2i$ genes, the first i genes are used to represent Network #1 and the others are for Network #2. For the convenience of connecting two networks, we fix the topology of the ith and $(i+1)$th genes as a thru-transmission line.

With this representation scheme, a multiplexer can be represented as a chromosome $\mathbf{g}$ (a set of structures). The design problem can be formulated as

$$\mathbf{g}^* = \arg\left(\min_{\mathbf{g}} U\left(\mathbf{S}\left(\mathbf{g}\right)\right)\right) \tag{1}$$

TABLE I
DETAILS OF THE BASIC ELEMENTS FOR THE GA

Category	Type	Name	Network Topology	Possible Connections	Electrical Parameters
Basic Circuit Elements	0	TL		Cascade and Parallel	Z_{o1} θ_1
	1	Sh_TL_OC		Cascade	Z_{o1} θ_1
	2	Sh_TL_SC		Cascade	Z_{o1} θ_1
	3	Sh_TL2_OC		Cascade	Z_{o1} θ_1 Z_{o2} θ_2
	4	Sh_TL2_SC		Cascade	Z_{o1} θ_1 Z_{o2} θ_2
Special Element	100	Empty		Cascade	None

Z_{oi}: characteristic impedance of the ith transmission line section.
θ_i: electrical length concerned at f_0 of the ith transmission line section in degrees.

where $\mathbf{S}(\mathbf{g})$ is the scattering matrix calculated by simple transmission-line models and $\mathbf{g}^*$ is the solution. Function U is the fitness function to be minimized, which is defined as

$$U = \left[(\Delta S_{22})^2 + (\Delta S_{33})^2 + (\Delta S_{21})^2 + (\Delta S_{31})^2\right]^{1/2} \tag{2}$$

$$\Delta S = \sum_{i=1}^{N} w_i f_i. \tag{3}$$

In (2), ΔS_{22}, ΔS_{33}, ΔS_{21}, and ΔS_{31} are the scores for optimization goals. In (3), w_i represents the weighting at the ith sampling point, f_i is the square of the difference between the magnitude of the calculated and the desired frequency responses at the ith sampling point, and N is the number of sampling points. Note that the magnitude of the frequency response is in decibel scale. The original fitness value of a chromosome is adjusted according to the fitness-sharing and fitness-scaling algorithms [19] in order to keep the diversity of chromosomes in a generation. The algorithm based on conventional GAs with one-point crossover and step-mutation operations [21] is then used to search for the chromosome whose frequency response meets the specifications of the desired multiplexer.

III. IMPLEMENTATION

Here, we design and implement a multiplexer for UWB and WLAN coexistence. The desired frequency response is described by piecewise-linear functions in Fig. 6, where the weighting of each linear region is also depicted. For a sampling point within the shading portions in this figure, the score of the point is set to zero if the evaluated value is smaller than the desired one. The multiplexer is desired to possess two passbands from 2.1 to 2.9 GHz and from 5.1 to 5.9 GHz for the WLAN at port 2 and two passbands from 3.1 to 4.9 GHz and from 6.1 to 8.2 GHz for the UWB at port 3 where the lower and higher bands are elaborately selected for Groups A and C in the MB-OFDM UWB system, respectively. Besides, the lower band at port 3 also covers the low-band of the DS-SS UWB system.

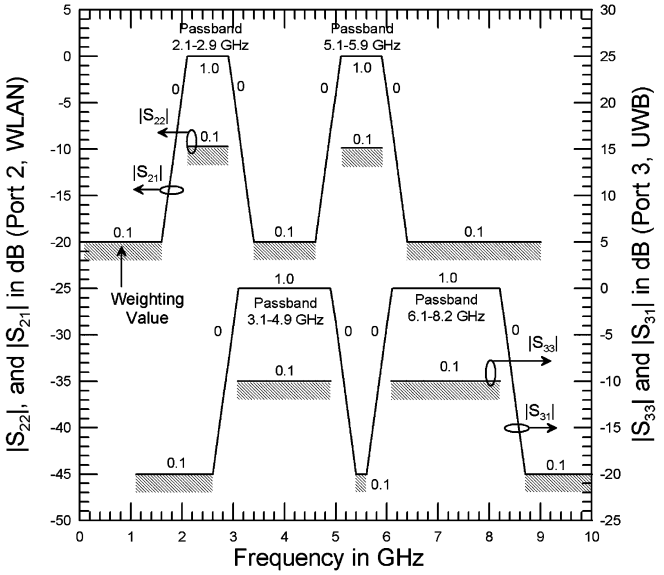

Fig. 6. Desired frequency response of the multiplexer.

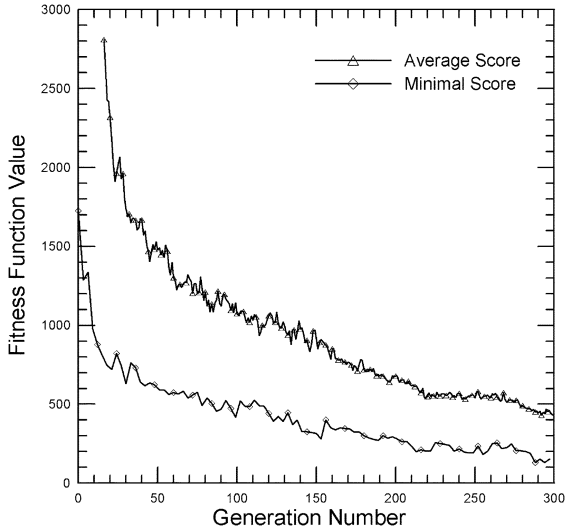

Fig. 7. Convergence of the GA.

The substrate used is an RO4003 with thickness $h = 0.508$ mm and relative dielectric constant $\varepsilon_r = 3.38$. Some constraints are added such that the transmission-line length and impedance in a basic circuit element should be within a reasonable range for the given substrate and only step-, tee-, and cross-junctions are accepted during synthesis. The population size in a generation is 300 and a chromosome is composed of 24 genes. The probabilities of crossover and mutation operator are 0.6 and 0.3, respectively.

Fig. 7 shows the convergence of the GA, where the average and minimal scores are without applying the fitness and sharing algorithms. After 300 generations evolution, the best chromosome consists of seven *Empty* elements, seven thru transmission lines, and ten stubs. The search takes approximately 3 min on a personal computer with a 2.4-GHz microprocessor. Next, the achieved electrical parameters are then converted to a physical circuit. Table II lists the electrical and physical parameters. The

TABLE II
ELECTRICAL AND PHYSICAL PARAMETERS OF THE MULTIPLEXER

No.	Name	Electrical Parameters (at f_0=4GHz)				Physical Parameters in mm (before tuning)			
		Z_{o1}	θ_1	Z_{o2}	θ_2	W_1	L_1	W_2	L_2
1	Empty	-	-	-	-	-	-	-	-
2	Empty	-	-	-	-	-	-	-	-
3	Empty	-	-	-	-	-	-	-	-
4	Empty	-	-	-	-	-	-	-	-
5	Sh_TL_SC	65.64	77.27	-	-	1.15	10.00	-	-
6	TL	40.00	20.10	-	-	2.58	2.51	-	-
7	Sh_TL2_SC	40.00	93.57	57.54	100.10	2.58	11.70	1.46	12.83
8	TL	99.45	42.28	-	-	0.47	5.63	-	-
9	Sh_TL_SC	58.98	83.69	-	-	1.40	10.75	-	-
10	Empty	-	-	-	-	-	-	-	-
11	Sh_TL2_OC	45.71	22.91	97.38	96.82	2.11	2.89	0.49	12.87
12	TL	80.67	50.50	-	-	0.76	6.63	-	-
13	TL	47.66	69.88	-	-	1.98	8.84	-	-
14	Sh_TL_SC	91.17	47.13	-	-	0.58	6.24	-	-
15	Sh_TL2_SC	93.92	98.76	56.73	44.25	0.54	12.10	1.49	5.67
16	TL	64.83	43.01	-	-	1.18	5.56	-	-
17	Sh_TL_OC	101.87	20.1	-	-	0.44	2.68	-	-
18	TL	45.12	47.35	-	-	2.16	5.98	-	-
19	Sh_TL_SC	55.50	80.98	-	-	1.55	10.36	-	-
20	TL	40.39	27.38	-	-	2.55	3.43	-	-
21	Sh_TL_OC	40.25	29.24	-	-	2.56	3.66	-	-
22	Empty	-	-	-	-	-	-	-	-
23	Empty	-	-	-	-	-	-	-	-
24	Sh_TL_SC	72.52	26.57	-	-	0.95	3.46	-	-

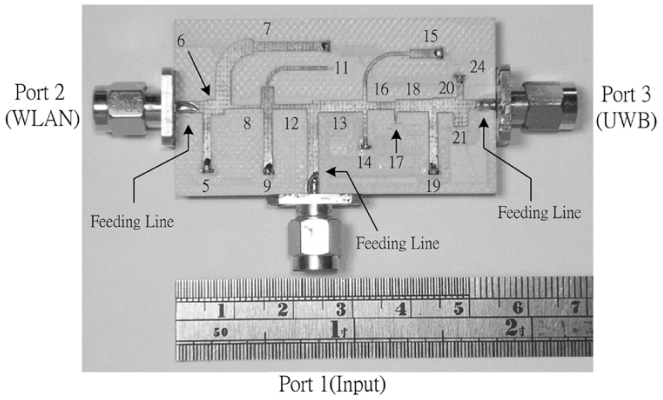

Fig. 8. Proposed multiplexer.

frequency response of the multiplexer with junction discontinuities is simulated again by the commercial circuit simulator Advanced Design System (ADS).[1] To count for the discontinuity effects, several physical parameters are slightly adjusted with the help of the commercial software. The size of the resultant multiplexer is 45 mm × 26 mm and its photograph is shown in Fig. 8, where the long stubs are bent to reduce the overall width of the circuit. Fig. 9 presents the simulated and measured scattering parameters. Note that $|S_{11}|$ is measured, while ports 2 and 3 are terminated in matched loads. It can be observed that the measured responses agree well with the simulated results.

According to the measured results, the multiplexer has two channels from 2.15 to 2.89 GHz and from 5.13 to 5.84 GHz at port 2, two channels from 3.22 to 4.83 GHz and from 6.07 to 8.22 GHz at port 3, and the isolations between ports 2 and 3 are better than 20 dB from dc to 2.03, 3.13 to 4.32, 5.24 to 5.53, and 6.76 to 10.0 GHz. The channel from 6.07 to 8.22 GHz is measured for a return loss better than 7.75 dB because the return loss is not very good between 6.0–7.0 GHz and the other channels are measured for a return loss better than 10 dB.

In Fig. 9(c), there is a small discrepancy in the measured and simulated $|S_{33}|$ between 6.0–7.0 GHz. It results from the grounding via-holes of the short-circuited stubs in the proposed multiplexer. When realizing the multiplexer, we retreat the location of the via-hole a distance approximately the height of the substrate in order to compensate the parasitic inductance introduced by the via-hole. This treatment corrects the locations of transmission poles contributed by a short-circuited stub. However, because it is a simple, but not very precise compensation, the treatment causes some influences on $|S_{33}|$.

IV. DISSCUSSIONS

A. Dual-Band Characteristic

To understand the circuit behaviors of the synthesized multiplexer, we decompose it into two two-port circuits and discuss the behaviors, respectively. The equivalent circuit of the WLAN part is described in Fig. 10, where the circuit can be regarded as a second-order DBR filter with a matching network near the input port. The input impedance $Z_{\text{in,UWB}}$ looking into the network can be represented as a large resistor in series with an inductor at 2.5 GHz and a lossy capacitor at 5.5 GHz. The DBR composed of elements 5–7 determines two transmission poles at 2.22 and 5.40 GHz and another DBR composed of elements 9 and 11 determines two transmission poles at 2.03 and 4.93 GHz. For the overall circuit, these poles shift to 2.79, 5.68, 2.28, and 5.20 GHz, respectively, making two poles inside the lower band and the other poles inside the higher band. Besides, we are also curious about the transmission zeros. Since each stub in a DBR filter brings its own transmission zeros depending on its resonant condition, the zeros can be easily found by letting $Z = 0$, where Z is the input impedance looking into the open- or short-circuited stub. As a result, we find that three zeros at 3.34, 8.60, and 9.32 GHz result from the elements 11, 9 and 5, respectively, and two zeros at 3.74 and 7.39 GHz stem from element 7. These poles and zeros make the DBR filter having the desired dual-band characteristic.

Similarly, the equivalent circuit of the UWB part is presented in Fig. 11. The input impedance $Z_{\text{in,WLAN}}$ can be represented as a large resistor in series with a capacitor at 4.5 GHz, a lossy capacitor at 3.5 GHz, and a lossy inductor at 3.5, 4.0, 6.5, 7.0, and 7.5 GHz. Next, we identify that two zeros at 5.40 and 9.78 GHz result from element 15 and one zero at 8.80 GHz stems from element 19. For the transmission poles, the DBR composed of elements 14 and 15 determines two poles at 4.08 and 7.58 GHz and the DBR comprised of elements 21 and 24 brings one pole at 5.23 GHz. It is difficult to intuitively identify the other poles because the other stubs do not arrange as fundamental DBR structures [15]–[17]. According to Fig. 9(c), it is seen that there are two poles inside the lower passband at 3.32 and 4.38 GHz and two poles inside the higher passband at 6.84 and 7.96 GHz. Consequently, we can say that the filter performance of the UWB part approximates a second-order BDR filter.

[1]Advanced Design System, Agilent Technol., Palo Alto, CA.

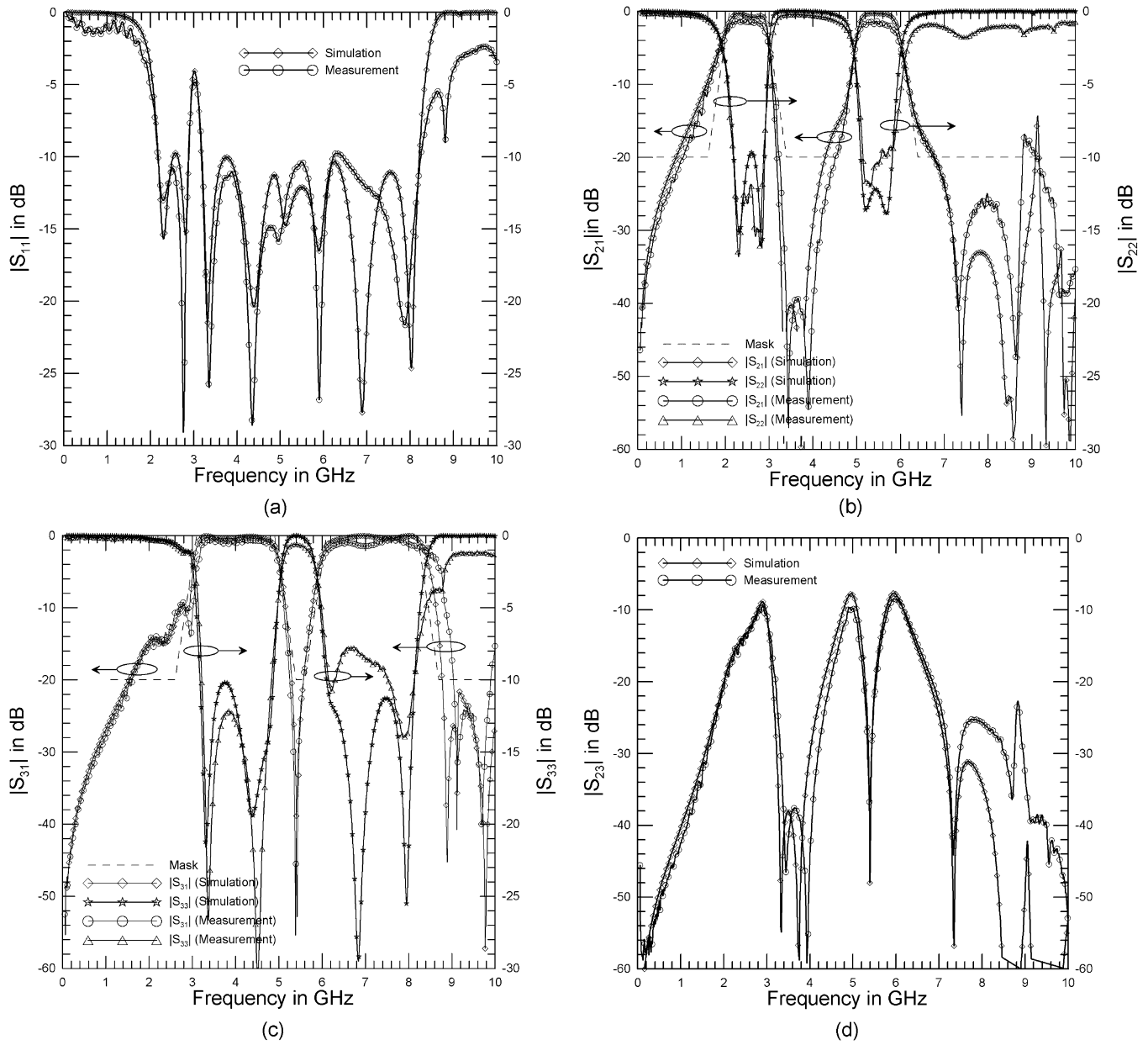

Fig. 9. Simulated and measured frequency responses of the designed multiplexer in decibels. (a) Magnitude of S_{11}. (b) Magnitude of S_{21} and S_{22}. (c) Magnitude of S_{31} and S_{33}. (d) Magnitude of S_{32}.

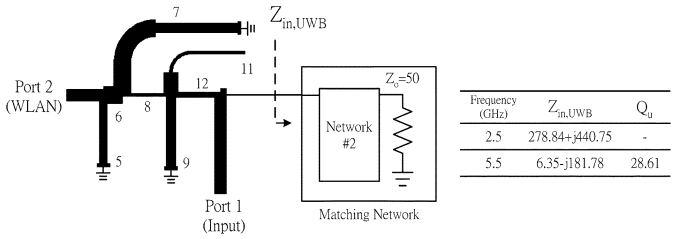

Frequency (GHz)	$Z_{in,UWB}$	Q_u
2.5	278.84+j440.75	-
5.5	6.35-j181.78	28.61

Fig. 10. Equivalent circuit of port 2.

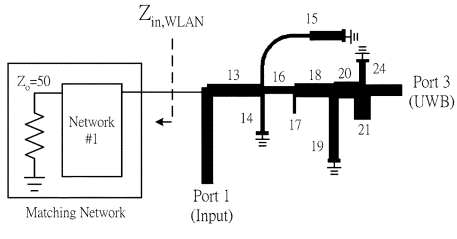

Frequency (GHz)	$Z_{in,WLAN}$	Q_u
3.5	0.03+j94.78	3159
4.0	1.00+j207.37	207.37
4.5	314.24-j671.16	-
6.5	8.10+j118.81	14.67
7.0	3.65+j243.90	66.82
7.5	7.48+j834.45	111.56
8.0	4.58-j800.66	174.82

Fig. 11. Equivalent circuit of port 3.

The unloaded quality factor Q_u defined by $|\mathrm{Im}(Z_{\mathrm{in}})|/\mathrm{Re}(Z_{\mathrm{in}})$ [22] of the microstrip matching stubs or microstrip resonators is hundreds on the RO4003 substrate below 10 GHz. The Q_u of $Z_{\mathrm{in,WLAN}}$ and $Z_{\mathrm{in,UWB}}$, except at 2.5 and 4.5 GHz, are shown in Figs. 10 and 11, respectively. The Q_u are very low at 5.5 and 6.5 GHz. Therefore, in Fig. 9(b) and (c), the insertion losses around these frequencies are not very good.

B. Isolation Issues Between WLAN and UWB Ports

As several radio transceivers coexist in a device, many unwanted interferences such as antenna-coupling noise, coupling

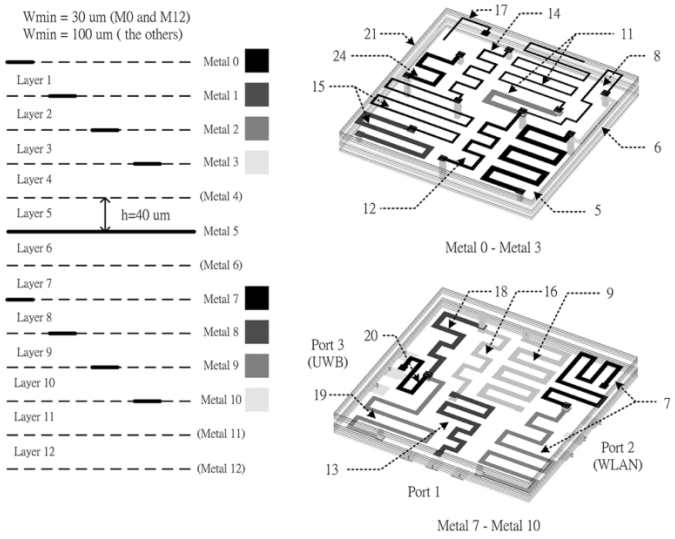

Fig. 12. Demonstration of the LTCC design.

noise on board, etc. should be considered. In a single-antenna configuration, there is no antenna-coupling noise. Assume that the circuit board can provide enough isolation between transceivers. Consequently, the main coupling path is through the multiplexer. In Fig. 9(d), the proposed multiplexer on average has an isolation of 10 dB from 2.0 to 3.0 GHz and from 5.0 to 6.0 GHz and an isolation of 20 dB from 3.0 to 5.0 GHz and from 6.0 to 10.0 GHz. The output powers of WLAN and MB-OFDM UWB transmitters are approximately 20 and -5 dBm [1], respectively. Assume that WLAN and UWB receivers can handle an input signal level smaller than -30 dBm. As a result, to make both receivers work well, the WLAN pre-selected filter requires an attenuation of 15 dB $(-5-10+30)$ from 3.0 to 5.0 GHz and 6.0 to 10.0 GHz and the UWB pre-selected filter requires an attenuation of 30 dB $(20-20+30)$ from 2.0 to 3.0 GHz and 5.0 to 6.0 GHz.

C. Problem on the Size of the Multiplexer

The size of the proposed multiplexer is 45 mm $\times$ 26 mm, seeming impractical for portable wireless facilities. However, size reduction can be accomplished by using a substrate with a higher dielectric constant such as an RO6010 with a 10.2 dielectric constant or a ceramic substrate. Furthermore, a miniature multiplexer could be implemented by folding the microstrip lines and using a laminated multilayer printed circuit board or a low-temperature co-fired ceramic (LTCC) process.

We demonstrate a design example based on LTCC using SONNET software[2] in Fig. 12, where a routing plan is plotted on the right-hand side of this figure. The LTCC used is composed of 12 layers, where each layer has a thickness $h = 40\ \mu$m and relative dielectric constant $\varepsilon_r = 7.8$. Metal 5 is designed as a ground plane, Metals 11 and 12 are reserved for routing in order to avoid the effect of characteristic impedance detuning while a LTCC circuit is assembled on a circuit board, and the others are for transmission-line routing. To reduce adjacent coupling effects, the minimal spacing between traces is set to $2h'$, where h' is the height from a trace to the ground plane. The overall volume is 5 mm $\times$ 5 mm $\times$ 0.48 mm, which is excellent for portable electronic facilities. Since such a design involves various parasitic effects such as corners, junctions, via-holes, etc., it is necessary to slightly tune the circuit parameters with the help of the full-wave numerical analysis. Besides, fabrication tolerances should also be carefully considered in the LTCC design.

[2]SONNET v9.52, SONNET Software Inc., Syracuse, NY.

V. Conclusions

In this paper, we have designed a novel microstrip three-port and four-channel multiplexer for WLAN and UWB coexistence, which is useful for portable wireless applications. The measured responses agree well with the simulations. The analysis of circuit behaviors, the problem regarding the size of the proposed multiplexer, and the isolation issues between WLAN and UWB ports have also been discussed. Additionally, the proposed algorithm can be used to synthesize other multiplexers in various multifunctional transceiver systems.

Acknowledgment

The circuit was fabricated and measured at National Chiao Tung University, Hsinchu, Taiwan, R.O.C. The authors wish to express their gratitude to Prof. R.-B. Hwang, National Chiao Tung University, and Prof. E.-Y. Chang, National Chiao Tung University, for their generous supports in experiments. Moreover, this paper owes much to the thoughtful and helpful comments of Prof. J.-D. Tseng, National Chin-Yi Institute of Technology, Taiping City, Taiwan, R.O.C.

References

[1] G. R. Aiello and G. D. Rogerson, "Ultra-wideband wireless systems," *IEEE Micro*, vol. 4, no. 2, pp. 36–47, Jun. 2003.
[2] B. Razavi, *RF Microelectronics*. Englewood Cliffs, NJ: Prentice-Hall, 1998, ch. 5.
[3] T.-G. Ma and S.-K. Jeng, "Planar miniature tapered-slot-fed annular slot antennas for ultrawide-band radios," *IEEE Trans. Antennas Propag.*, vol. 53, no. 3, pp. 1194–1202, Mar. 2005.
[4] A. K. Y. Lai, A. L. Sinopoli, and W. D. Burnside, "A novel antenna for ultra-wide-band applications," *IEEE Trans. Antennas Propag.*, vol. 40, no. 7, pp. 755–760, Jul. 1992.
[5] L. M. George, Y. Leo, and E. M. T. Jones, *Microwave Filters, Impedance-Matching Networks, and Coupling Structures*. New York: McGraw-Hill, 1964, ch. 16.
[6] G. L. Matthaei and E. G. Cristal, "Multiplexer channel-separation units using interdigital and parallel-coupled filters," *IEEE Trans. Microw. Theory Tech.*, vol. 13, no. 5, pp. 328–334, May 1965.
[7] R. J. Wenzel, "Printed-circuit complementary filters for narrow bandwidth multiplexers," *IEEE Trans. Microw. Theory Tech.*, vol. MTT-16, no. 3, pp. 147–157, Mar. 1968.
[8] M. A. Ismail, D. Smith, A. Panariello, Y. Wang, and M. Yu, "EM-based design of large-scale dielectric-resonator filters and multiplexers by space mapping," *IEEE Trans. Microw. Theory Tech.*, vol. 52, no. 1, pp. 386–392, Jan. 2004.
[9] A. Garcia-Lamperez, S. Llorente-Romano, M. Salazar-Palma, and T. K. Sarkar, "Efficient electromagnetic optimization of microwave filters and multiplexers using rational models," *IEEE Trans. Microw. Theory Tech.*, vol. 52, no. 2, pp. 508–521, Feb. 2004.
[10] S. Srisathit, S. Patisang, R. Phromloungsri, S. Bunnjaweht, S. Kosulvit, and M. Chongcheawchamnan, "High isolation and compact size microstrip hairpin diplexer," *IEEE Microw. Wireless Compon. Lett.*, vol. 15, no. 2, pp. 101–103, Feb. 2005.
[11] J.-W. Sheen, "LTCC-MLC duplexer for DCS," *IEEE Trans. Microw. Theory Tech.*, vol. 47, no. 9, pp. 1883–1890, Sep. 1999.

[12] B. Strassner and K. Chang, "Wide-band low-loss high-isolation microstrip periodic-stub diplexer for multiple-frequency applications," *IEEE Trans. Microw. Theory Tech.*, vol. 49, no. 3, pp. 1818–1820, Mar. 2001.
[13] T.-Y. Yun, C. Wang, P. Zepeda, C. T. Rodenbeck, M. R. Coutant, M.-Y. Li , and K. Chang, "A 10- to 21-GHz low-cost, multifrequency, and full-duplex phased-array antenna system," *IEEE Trans. Antennas Propag.*, vol. 50, no. 5, pp. 641–650, May 2002.
[14] R. Levy, R. V. Snyder, and G. Matthaei, "Design of microwave filters," *IEEE Trans. Microw. Theory Tech.*, vol. 50, no. 4, pp. 783–793, Apr. 2002.
[15] C. Quendo, E. Rius, and C. Person, "Narrow bandpass filters using dual-behavior resonators," *IEEE Trans. Microw. Theory Tech.*, vol. 51, no. 3, pp. 734–743, Mar. 2003.
[16] ——, "Narrow bandpass filters using dual-behavior resonators based on stepped-impedance stubs and different-length stubs," *IEEE Trans. Microw. Theory Tech.*, vol. 52, no. 3, pp. 1034–1044, Mar. 2004.
[17] G. Prigent, E. Rius, F. Le Pennec, S. Le Maguer, C. Quendo, G. Six, and H. Happy, "Design of narrow-band DBR planar filters in Si–BCB technology for millimeter-wave applications," *IEEE Trans. Microw. Theory Tech.*, vol. 52, no. 3, pp. 1045–1051, Mar. 2004.
[18] D. E. Goldberg, *Genetic Algorithms in Search Optimization & Machine Learning*. Reading, MA: Addison-Wesley, 1989.
[19] M. Gen and R. Cheng, *Genetic Algorithms & Engineering Optimization*. New York: Wiley, 2000, ch. 1–3.
[20] Y. Ruhmat-Samii and E. Michielssen, *Electromagnetic Optimization by Genetic Algorithms*. New York: Wiley, 1999.
[21] A. E. Eiben, R. Hinterding, and Z. Michalewicz, "Parameter control in evolutionary algorithm," *IEEE Trans. Evol. Comput.*, vol. 3, no. 2, pp. 124–141, Jul. 1999.
[22] G. M. Rebeiz, *RF MEMS Theory, Design, and Technology*. New York: Wiley, 2003, ch. 11.

Ming-Iu Lai (S'04) was born in Kaohsiung, Taiwan, R.O.C., in 1976. He received the B.S.E.E. degree from National Taiwan University of Science and Technology, Taipei, Taiwan, R.O.C., in 1998, the M.S.E.E. degree from National Taiwan University, Taipei, Taiwan, R.O.C., in 2000, and is currently working toward the Ph.D. degree at National Taiwan University.

From 2001 to 2002, he was with the ZyXEL Communication Corporation, Hsinchu, Taiwan, R.O.C., where he was involved with signal integrity (SI) and electromagnetic interference (EMI) analyses. From 2002 to 2004, he was with the SynComm Communication Corporation, Hsinchu, Taiwan, R.O.C., and then joined the Applied Electromagnetic Research Laboratory, Microelectronics and Information System Research Center, National Chiao Tung University, Hsinchu, Taiwan, R.O.C., where he was involved with the designs of beam-steering antennas and high-frequency flip-chip packages. His current research interest includes two-dimensional/three-dimensional (2-D/3-D) microwave circuits design automation, grid computing techniques, and GAs for electromagnetic optimization designs, and time-domain numerical electromagnetics.

Shyh-Kang Jeng (M'86–SM'98) received the B.S.E.E. and Ph.D. degrees from National Taiwan University, Taipei, Taiwan, R.O.C., in 1979 and 1983, respectively.

In 1981, he joined the faculty of the Department of Electrical Engineering, National Taiwan University, where he is currently a Professor. From 1985 to 1993, he was with the University of Illinois at Urbana-Champaign, as a Visiting Research Associate Professor and a Visiting Research Professor. In 1999, he was with the Center for Computer Research in Music and Acoustics, Stanford University, Stanford, CA, for six months. His research interest includes numerical electromagnetics, UWB wireless systems, music signal processing, music information retrieval, intelligent agent applications, and electromagnetic scattering analysis.